PROCEEDINGS OF SCIENCE

Data-driven Estimation of Invisible Energy below EeV

Jakub Vícha,[a,*] **Vladimír Novotný**[a] **and Jan Ebr**[a]

[a] *Institute of Physics of the Czech Academy of Sciences,*
Na Slovance 1999/2, Prague, Czech republic

E-mail: vicha@fzu.cz

The calorimetric energy of a cosmic-ray shower is measured by optical telescopes from the emission of isotropic fluorescence light or from the collimated Cherenkov light through the number of charged secondary particles. To reconstruct the energy of the primary cosmic ray the calorimetric energy needs to be further corrected for the energy that is not deposited in the atmosphere. This invisible energy is a substantial source of systematic uncertainties in the energy spectrum of cosmic rays measured by optical telescopes below 1 EeV. Usually, estimations of the invisible energy below 1 EeV relied on Monte Carlo simulations despite the fact that models of hadronic interactions have problems in describing the measured air-shower data. We apply a data-driven method to derive the invisible energy for air showers using the publicly available data of the KASCADE and IceTop experiments. The universal relation between the invisible energy and the number of muons measured by the detectors was utilized. In this way, we determine the invisible energy from measured data between PeV and EeV energies and compare with invisible-energy models adopted at the Pierre Auger and Telescope Array observatories.

38th International Cosmic Ray Conference (ICRC2023)
26 July - 3 August, 2023
Nagoya, Japan

ICRC2023
38th International Cosmic Ray Conference
The Astroparticle Physics Conference

*Speaker

© Copyright owned by the author(s) under the terms of the Creative Commons Attribution-NonCommercial-NoDerivatives 4.0 International License (CC BY-NC-ND 4.0).

PoS(ICRC2023)497

1. Introduction

VHECR (Very-high energy cosmic rays) are charged particles in the energy range 10^{15-18} eV. When the VHECR energy is measured using fluorescence telescopes [1–3], the measured calorimetric energy must be corrected for the energy that is not deposited in the atmosphere. This so-called invisible energy is carried by muons and neutrinos, and is a substantial source of systematic uncertainties in the energy spectrum measured by optical telescopes below 1 EeV (in case of Telescope Array experiment ∼10% [3], in case of Auger experiment ∼8% [4]).

The invisible energy of VHECR is usually estimated from simulations for a given mass composition of VHECR despite the fact that HI models have problems to describe the measured air-shower data and, therefore, also the mass composition of VHECR is burdened by high systematic uncertainties. The problems of HI models tuned to the LHC data to describe air-shower data of VHECR (especially the muon component of shower) were reported in [5] for KASCADE-Grande. The inconsistency of description of measured muons using MC simulations is higher at ultra-high energies (above 1 EeV) [6–8].

At the ultra-high energies, a data-driven method was applied to the hybrid data of fluorescence and ground detectors of the Pierre Auger Observatory above $10^{18.6}$ eV and extrapolated down to 10^{17} eV [9], where also a phenomenological description of the data-driven method can be found. This way, the invisible energy was found to be even larger than the MC simulations predict for iron nuclei.

In this work, we apply a data-driven method to derive the invisible energy from the publicly available VHECR data of the KASCADE and IceTop experiments [10, 11]. The universal relation between the invisible energy and the number of muons measured by the shielded KASCADE detectors was derived and adopted. We also use IceTop data to estimate the energy evolution of invisible energy. In this way, we determine the invisible energy from measured data between PeV and EeV energies and compare with models of invisible energy adopted by Telescope Array and Pierre Auger Observatory.

2. KASCADE Data and Simulations

The KASCADE experiment [12] measured VHECR since 1996 and finished its measurement in 2003. The detected showers were reconstructed using signals in shielded (signals dominantly from muons above 230 MeV) and unshielded scintillation detectors (signals from charged particles). The collected data of this experiment were recently released together with simulations at the reconstruction level including the detector effects [10] accessible from [13].

Both simulated and measured data contain information on the reconstructed number of muons on ground with energy threshold 230 MeV (N_μ^{Rec}), the zenith angle (Θ_{Rec}), the lateral shape parameter (s^{Rec}), and the shower energy (E_{Rec}). The KASCADE simulations contain additionally to the reconstructed quantities also the true information on the number of muons above 100 MeV (N_μ^{MC}), the number of of electrons ($N_{\mathrm{el}}^{\mathrm{Rec}}$), the true zenith angle (Θ^{MC}), primary energy (E_{MC}) and the type of primary particle initiating the generated shower. However these KASCADE simulations do not include information on the calorimetric or invisible energy. Therefore, we produced an additional library of showers simulated in program CORSIKA [14] with the same settings as the

PoS(ICRC2023)497

publicly available KASCADE simulations to obtain the information on the invisible energy (E_{Inv}) and to finally relate it with the number of generated muons.

2.1 KASCADE Data

We used NABOO 2.0 version [10] of released data for runs 4685-7417 containing 252,658,250 reconstructed showers from period 08.05.1998 – 20.12.2003 with zenith angle Θ_{Rec} = 0°-60°, azimuth angle 0°-360°, lateral shape parameter s^{Rec} = 0.1-1.48, core positions in the square of size 91 m centred in the middle of the KASCADE experiment with $\log_{10} N_{\mathrm{el}}^{\mathrm{Rec}}$ and $\log_{10} N_{\mu}^{\mathrm{Rec}}$ both higher than 2. This pre-selection of data guarantees a constant quality of the measured data.

To the preselected data set, we applied cuts on the reconstructed numbers of particles $\log_{10} N_{\mathrm{el}}^{\mathrm{CUT}}$ = 4.4 and $\log_{10} N_{\mu}^{\mathrm{CUT}}$ = 4.0. We applied also additional cuts recommended by the KASCADE group to maintain high quality of the reconstructed data [15]: $s_{\mathrm{low}}^{\mathrm{CUT}} = 0.6$, $s_{\mathrm{high}}^{\mathrm{CUT}} = 1.3$ to cut finally showers with $\log_{10} N_{\mathrm{el}}^{\mathrm{Rec}} < \log_{10} N_{\mathrm{el}}^{\mathrm{CUT}}$, $\log_{10} N_{\mu}^{\mathrm{Rec}} < \log_{10} N_{\mu}^{\mathrm{CUT}}$, and $s^{\mathrm{Rec}} < s_{\mathrm{low}}^{\mathrm{CUT}}$ and $s^{\mathrm{Rec}} > s_{\mathrm{high}}^{\mathrm{CUT}}$.

For our analysis, we use only showers with $\Theta_{\mathrm{Rec}} \leq 25°$ since the formula for estimation of the shower energy using $\log_{10} N_{\mathrm{el}}^{\mathrm{Rec}}$ and $\log_{10} N_{\mu}^{\mathrm{Rec}}$ was derived for $\Theta^{\mathrm{MC}} \leq 25°$ [10]. Finally, 16,302,464 measured showers were used to calculate the invisible energy from the measured number of muons.

2.2 KASCADE Simulations

The publicly available simulations are described in see [16]. The energy of primary particles followed an energy spectrum with spectral index $\gamma_{\mathrm{MC}} = 2$ from 10^{14} eV to 10^{18} eV; with high-energy extension to $3.16 \cdot 10^{18}$ eV. For the purpose of our analysis, we reweighted the simulated showers to correspond to the energy spectrum of measured data with spectral index ~2.7. In our analysis, we use showers simulated with EPOS-LHC [17], QGSJet II-04 [18] and Sibyll 2.3 [19] to estimate reconstruction biases on N_{μ}^{Rec} and E_{Rec} for p, He, C and Fe primaries. The energy cut-off for electrons, photons and neutral pions was set to 3 MeV and for muons and hadrons to 100 MeV [16].

The same cuts as the cuts applied to the set of measured data were applied to these simulations, except $s_{\mathrm{low}}^{\mathrm{CUT}} = 0.0$ as recommended by the KCDC group [16]. We checked that these cuts keep full reconstruction efficiency of all primary particles above the shower energy $10^{15.3}$ eV.

Finally, we have obtained about 30,000 selected showers of 500,000 showers at disposal for given model of hadronic interactions and primary particle within $\Theta_{\mathrm{MC}} = 25°$.

2.2.1 Unfolding Number of muons and Shower Energy

We derived from the KASCADE simulations the parametrization of the average bias on the reconstructed number of muons and on the reconstructed energy for showers with $\Theta_{\mathrm{MC}} \leq 25°$.

The average relative bias on the number of muons above 100 MeV, $\eta_{\mu} = \left(N_{\mu}^{\mathrm{Rec}} - N_{\mu}^{\mathrm{MC}}\right) / N_{\mu}^{\mathrm{MC}}$, was parametrized for each primary particle and each model of hadronic interactions with a polynomial of the 4$^{\mathrm{th}}$ order as a function of the reconstructed energy for each of the 4 zenith angle ranges dividing the zenith-angle range 0°-25° equidistantly in $\cos^2(\Theta_{\mathrm{MC}})$.

In case of the parametrization of the average relative bias depending on the reconstructed energy, $\eta_{\mathrm{E}} = (E_{\mathrm{Rec}} - E_{\mathrm{MC}}) / E_{\mathrm{MC}}$, a polynomial of the 3$^{\mathrm{rd}}$ order was used for $E_{\mathrm{Rec}} \geq 10^{15.3}$ eV. The dependence of polynomial coefficients on $\cos^2(\Theta_{\mathrm{MC}})$ for $\eta_{\mu}(E_{\mathrm{Rec}})$ and $\eta_{\mathrm{E}}(E_{\mathrm{Rec}})$ was assumed to be cubic.

PoS(ICRC2023)497

The reconstructed quantities were corrected for the average bias on event-by-event basis for given mass composition with primary fractions f_i, $\sum_i f_i = 1$ for i = p, He, C, Fe as $N_\mu = N_\mu^{\mathrm{Rec}}/\sum_i(f_i \cdot \eta_\mu(E_{\mathrm{Rec}}))$, and $E_{\mathrm{Tot}} = E_{\mathrm{Rec}}/\sum_i(f_i \cdot \eta_{\mathrm{E}}(E_{\mathrm{Rec}}))$. The maximal values of the mean residuals after the application of the bias corrections for individual primaries and fro HI models are a substantial source of systematic uncertainty in the final results (see Section 2.5).

2.3 Additional CORSIKA Simulations

We produced 60,000 showers using CORSIKA 7.6400 using three HI models, EPOS-LHC, QGSJet II-04 and Sibyll 2.3 (the same as in case of the KASCADE simulations), and low-energy model FLUKA 2011.2x for 4 primary particles: p, He, N and Fe. Ten fixed values of the zenith angle were distributed uniformly in $\cos^2\Theta_{\mathrm{MC}}$ (Θ_{MC}=0°, 12.3°, 17.6°, 21.8°, 25.4°, 28.6°, 31.7°, 34.5°, 37.3° and 40°) for each of 5 fixed primary energies (E_{MC}=10^{15} eV, $3.2{\cdot}10^{15}$ eV, 10^{16} eV, $3.2{\cdot}10^{16.5}$ eV and 10^{17} eV). For each model of hadronic interactions, primary particle, energy and zenith angle, 100 showers were generated. The settings of CORSIKA simulations were adjusted according to the settings mentioned in Sec. 2.2.

The calorimetric energy (E_{Cal}) was calculated for each simulated shower as the sum of energy deposited by charged particles at each depth of shower until the ground level. A correction for a part of the calorimetric energy below the ground was accounted for. The invisible energy was then obtained as $E_{\mathrm{Inv}} = E_{\mathrm{MC}} - E_{\mathrm{Cal}}$. The number of muons ($N_\mu^{\mathrm{MC}}$) was obtained as a sum of all muons (above 100 MeV) reaching the ground level as in the case of N_μ^{MC} in KASCADE simulations. The difference of $\langle N_\mu^{\mathrm{MC}}\rangle$ between KASCADE simulations and additional CORSIKA simulations was found to be within 0.5% (see also large markers in Fig. 1).

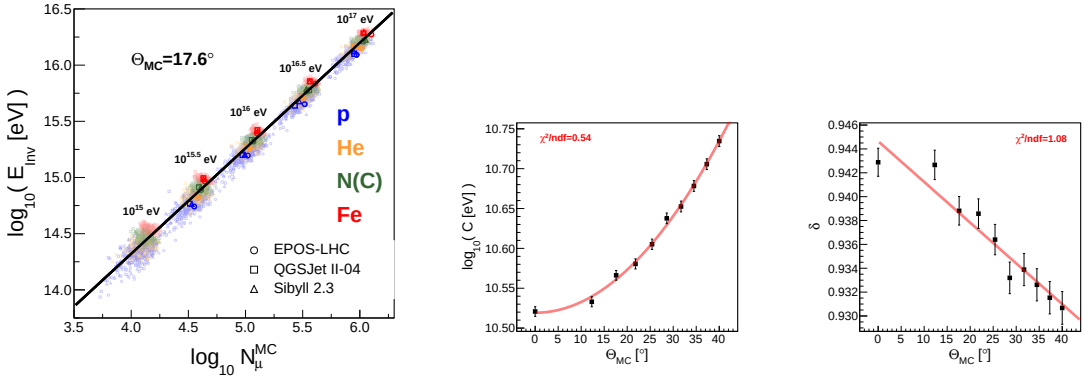

Figure 1: Left: Relation between the invisible energy (E_{Inv}) and the number of muons above 100 MeV (N_μ^{MC}). The individual showers of additional CORSIKA simulations (small markers) generated for 5 fixed energies and the zenith angle Θ_{MC} = 17.6° that were used for the fit (black line). The larger markers are estimations of $\langle N_\mu^{\mathrm{MC}}\rangle$ from KASCADE simulations (p, He, C, Fe) for narrow ranges of energy and the zenith angle around the fixed values of additional CORSIKA simulations vs. the corresponding $\langle E_{\mathrm{Inv}}\rangle$ of the additional CORSIKA simulations (p, He, N, Fe). Middle and right: Dependence of fitted parameters C (middle) and δ (right) on zenith angle. These dependencies were assumed to be quadratic and linear, respectively.

PoS(ICRC2023)497

2.4 Data-driven Method

The additional CORSIKA simulations were used to calibrate $E_{\rm Inv}$ with $N_\mu^{\rm MC}$ for each of ten fixed zenith angles (see an example on the left panel of Fig. 1 for $\Theta_{\rm MC} = 17.6°$) according to $E_{\rm Inv} = C \cdot \left(N_\mu^{\rm MC}\right)^\delta$. The showers of all three HI models, all four primaries and all five energy bins were fitted with the least square method. The obtained parameters C and δ are depicted on the middle and right panel of Fig. 1, respectively, for different $\Theta_{\rm MC}$. The zenith angle dependencies of parameters C and δ were fitted with quadratic and linear functions, respectively, using the least square method: $\log_{10}(C\ [\mathrm{eV}]) = c_0 + c_1 \cdot (\Theta_{\rm MC}[°]) + c_2 \cdot (\Theta_{\rm MC}[°])^2$, $\delta = d_0 + d_1 \cdot (\Theta_{\rm MC}[°])$. These dependencies come mainly from the attenuation of $N_\mu^{\rm MC}$. The difference of $E_{\rm Inv}$ between $\Theta_{\rm MC}$=0° and $\Theta_{\rm MC}$=25° was found to be within ~2%.

In the following, the relation between $E_{\rm Inv}$ and $N_\mu^{\rm MC}$ was considered universal with respect to the HI model and the mass composition of primary particles. The maximal residuals of fitted $E_{\rm Inv}$ ($\Delta E_{\rm Inv}/E_{\rm Inv}$) contribute significantly to the total systematic uncertainty of the results (see Section 2.5 and the right panel of Fig. 2 for more details).

For showers of ultra-high energies detected by hybrid detectors of the Pierre Auger Observatory [9], $E_{\rm Cal}$ was measured directly by fluorescence telescopes with very low systematic uncertainties at the level of 14%. $E_{\rm Inv}$ was measured independently using ground detectors and then related to the $E_{\rm Cal}$ for the same showers. An estimate of the $E_{\rm Inv}$ applicable to the optical measurements was provided in the form of $E_{\rm Inv}/E_{\rm Tot} = E_{\rm Inv}/E_{\rm Tot}(\log_{10}(E_{\rm Cal}\ [\mathrm{eV}])$.

In case of the KASCADE experiment, the shower energy ($E_{\rm Rec}$) is estimated from the measured number of muons and electrons on ground [10]. It is based on the comparison with signals of showers generated by given energy for HI model QGSJet II-02 and Fluka 2002_4. Such energy calibration is substantially biased wrt. the mass composition and HI models (up to 50-10% for energies $10^{15.5-18.0}$ eV). Therefore, we present our results for a combination of the 4 primaries (p, He, C and Fe) developing with the shower energy according to the Global Spline Fit (GSF) model [20] for primary fractions of p, He, CNO group and Fe group, respectively. We applied a rescaling of the energy scale in GSF by 0.88 to account for the energy rescaling applied in [20] for KASCADE-Grande that we consider to have the same energy scale as the KASCADE experiment (energy calibrations using the same MC simulations).

For each shower reconstructed with zenith angle $\Theta_{\rm Rec}$, $N_\mu^{\rm Rec}$ and $E_{\rm Rec}$, the number of muons on ground (N_μ) and the shower energy ($E_{\rm Tot}$) are obtained for primary fractions predicted by the GSF model at average unfolded energy $\langle E_{\rm Tot}\rangle$. This energy is calculated bias correction for all primary fractions 25%. The invisible energy, $E_{\rm Inv}\left(N_\mu\right)$, is calculated for $C(\Theta_{\rm Rec})$ and $\delta(\Theta_{\rm Rec})$ for the corresponding zenith angle. We derive $E_{\rm Cal}$ as $E_{\rm Cal} = E_{\rm Tot} - E_{\rm Inv}$.

2.5 Systematic Uncertainties

We consider several sources of systematic uncertainty in our method contributing to the total systematic uncertainty at a level of 20% of $E_{\rm Inv}/E_{\rm Tot}$ (see the right panel of Fig. 2). The individual contributions of the systematic uncertainties of $E_{\rm Inv}$ and $E_{\rm Tot}$ were summed in quadrature and propagated to the total systematic uncertainty of $E_{\rm Inv}/E_{\rm Tot}$.

The main contribution to the systematic uncertainty of $E_{\rm Inv}$ comes from the quasi-universal calibration (left panel of Fig. 1) of $E_{\rm Inv}$ with $N_\mu^{\rm MC}$. The residual dependence ($\Delta E_{\rm Inv}/E_{\rm Inv}$) on HI

PoS(ICRC2023)497

model and mass composition decreases from $\sim \pm 20\%$ at $10^{15.5}$ eV to $\sim \pm 15\%$ at 10^{17} eV mainly due to decreasing shower-to-shower fluctuations with increasing energy of showers. The decreasing trend of this uncertainty was extrapolated beyond the energy 10^{17} eV where a reasonable amount of data is present, but not of simulations to be confirmed.

The systematic uncertainty of E_{Inv} stemming from the imperfection of the parameterization of the N_μ bias η_μ was estimated to increase from $\Delta E_{\mathrm{Inv}}/E_{\mathrm{Inv}} \sim \pm 2\%$ to $\sim \pm 4\%$. The systematic uncertainty of E_{Tot} due to the bias correction η_{E} increases from $\Delta E_{\mathrm{Tot}}/E_{\mathrm{Tot}} \sim \pm 4\%$ at $10^{15.5}$ eV to $\sim \pm 15\%$ and $10^{17.5}$ eV. The increase of these uncertainties with energy is a consequence of the decrease of statistics in KASCADE simulations and therefore from the reduced reliability of the bias descriptions.

The relative difference in N_μ^{MC} between KASCADE simulations and the additional CORSIKA simulations was found to be around 0.5%. Such a difference is expected to come from different versions of CORSIKA and FLUKA. The remaining relative differences for individual primaries were found to be at a level of 5% (stemming predominantly from low statistics of simulations), which is a value included conservatively as the systematic uncertainty of E_{Inv} ($E_{\mathrm{Inv}} \propto N_\mu^{\mathrm{MC}}$).

The systematic uncertainty stemming from the mass composition adopting the GSF model was estimated as the largest change of the results when the proton and helium primary fractions were increased/decreased by 10%, and nitrogen and iron fractions were decreased/increased by 10% to obtain the lightest and the heaviest composition, respectively, from the four components adopting the uncertainty of primary fractions of 10%. The uncertainties of the mass composition derived with the GSF method were estimated to influence our results by few % as a result of different relative weights of the bias corrections for each of the four primaries.

3. IceTop Data

The invisible energy can also be estimated indirectly from the measurement of muon densities. This method is based on the relation $E_{\mathrm{Inv}} = \epsilon_\pi^{\mathrm{C}} \times N_\mu$ which comes from the Heitler–Matthews' model and was validated using detailed MC simulations [9]. N_μ is the number of muons in the extensive air shower reaching ground level, and $\epsilon_\pi^{\mathrm{C}}$ is the pion critical energy. If the corresponding MC simulations of the detector response are also available, the invisible energy can be obtained using [4]

$$E_{\mathrm{Inv}} = E_{\mathrm{Inv,p}} \left(\frac{E_{\mathrm{Inv,Fe}}}{E_{\mathrm{Inv,p}}} \right)^z, \qquad z = \frac{\ln(N_\mu^{\mathrm{det}}) - \ln(N_{\mu,\mathrm{p}}^{\mathrm{det}})}{\ln(N_{\mu,\mathrm{Fe}}^{\mathrm{det}}) - \ln(N_{\mu,\mathrm{p}}^{\mathrm{det}})},$$

where $E_{\mathrm{inv,p}}$ and $E_{\mathrm{inv,Fe}}$ are the invisible energies estimated by the chosen high–energy interaction model, here QGSJetII-04, for protons and iron nuclei, respectively. The quantity z can be estimated e.g. from the IceTop data [11] as was done in [21].

4. Comparison of Results with Invisible-energy Models

On the left panel of Fig. 2, the mean fractions of the invisible energy to the shower energy from KASCADE data are plotted for each of the three HI models as a function of the logarithm of the calorimetric energy. Due to the strong dependence of E_{Tot} on primary mass (up to ~50%) and HI model (up to ~20%), the resulting $E_{\mathrm{Inv}}/E_{\mathrm{Tot}}$ is plotted for the combination of primaries

PoS(ICRC2023)497

corresponding to the GSF model for each of the three HI models and the corresponding rescaling of the E_{Tot} by 0.88 according tothe GSF model was applied. For comparison, we plot the MC predictions for protons (blue) and iron nuclei (red) obtained with CONEX 6.40 [22, 23] simulations for zenith angles within 25° and energies between 10^{15} eV and 10^{20} eV. The IceTop data for two optimal shower-core distances are depicted as well. Finally, we plot the invisible-energy models adopted at the Pierre Auger [4] and Telescope Array [3] observatories.

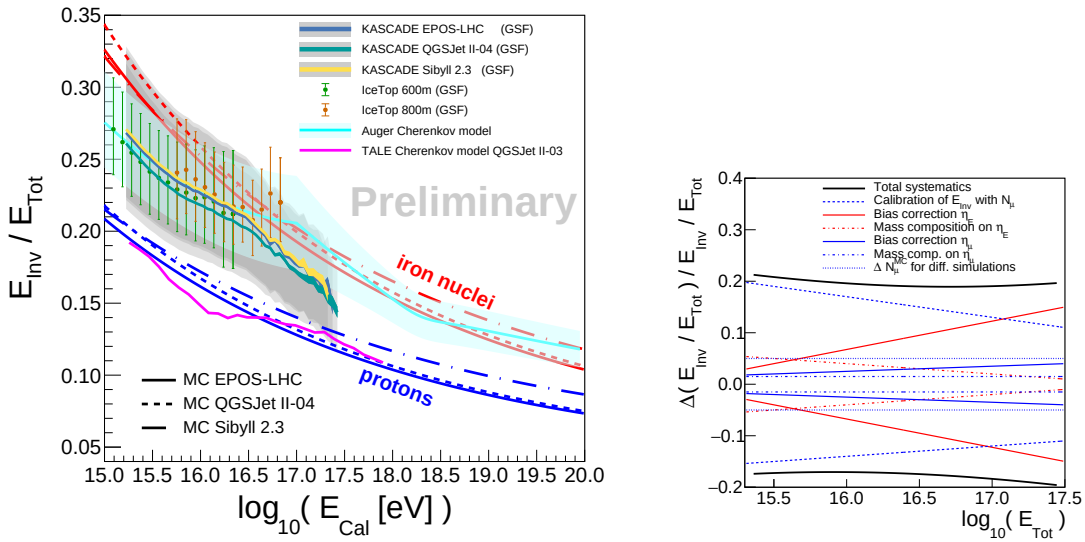

Figure 2: Left: Ratio of the invisible energy to the total shower energy as a function of the logarithm of calorimetric energy derived from KASCADE (systematics in gray bands) and IceTop data at two different shower-core distances. The models adopted at the Pierre Auger [4] and Telescope Array [3] observatories is depicted by cyan and purple lines, respectively. Right: Individual contributions to the total systematic uncertainty of the ratio of the invisible energy to the total shower energy for KASCADE data.

The Auger model includes extrapolation of the Auger measurements down to 10^{17} eV assuming the mass evolution according to the Auger measurements and no evolution of the muon discrepancy between data and simulations with energy. In the range of $\log_{10}(E_{\mathrm{Cal}}\ [\mathrm{eV}])= 17.0 - 17.4$, the measurement using KASCADE data is below the extrapolation of Auger measurements, athough still within the quoted systematic uncertainties. This difference might be a consequence of an energy evolution of the muon deficit in simulations, or by different energy scales adopted by the experiments that can be imprecisely accounted by the GSF model.

The energy spectrum measured by TALE optical telescopes between ∼2 PeV and ∼2 EeV [3] used prediction for energy evolution of the mass composition that matched the observed data on the depth of shower maximum (X_{max}), so called TXF composition model. Such comparison relies on the absolute scale of $\langle X_{\mathrm{max}} \rangle$ for given HI model, which is a subject of large systematic uncertainties (see e.g. [24]). Although not specified by TALE, we estimate from the quoted results that the TXF composition model predicts mass composition that is dominated by protons at most of the energies.

Our results using publicly available data of IceTop and KASCADE experiments suggest better accordance with the invisible-energy model adopted by the Pierre Auger Observatory.

PoS(ICRC2023)497

Acknowledgements

This work was supported by the Czech Science Foundation 21-02226M.

References

[1] J. Abraham et al. The fluorescence detector of the Pierre Auger Observatory. *NIM A*, 620(2):227 – 251, 2010.
[2] R. U. Abbasi et al. Study of Ultra-High Energy Cosmic Ray composition using Telescope Array's Middle Drum detector and surface array in hybrid mode. *Astropart. Phys.*, 64:49–62, 2015.
[3] R. U. Abbasi et al. The Cosmic Ray Energy Spectrum between 2 PeV and 2 EeV Observed with the TALE Detector in Monocular Mode. *The Astrophysical Journal*, 865(1):74, sep 2018.
[4] V. Novotný for the Pierre Auger Collaboration. Measurement of the spectrum of cosmic rays above $10^{16.5}$ eV with Cherenkov–dominated events at the Pierre Auger Observatory. *PoS*, ICRC2019:374, 2019.
[5] W.D. Apel et al. Probing the evolution of the EAS muon content in the atmosphere with KASCADE-Grande. *Astroparticle Physics*, 95:25 – 43, 2017.
[6] A. Aab et al. Testing Hadronic Interactions at Ultrahigh Energies with Air Showers Measured by the Pierre Auger Observatory. *Physics Review Letters*, 117:192001, Oct 2016.
[7] A. Aab et al. Muons in air showers at the Pierre Auger Observatory: Mean number in highly inclined events. *Phys. Rev. D*, 91:059901, Mar 2015.
[8] A. Aab et al. Erratum: Muons in air showers at the Pierre Auger Observatory: Measurement of atmospheric production depth [Phys. Rev. D 90, 012012 (2014)]. *Phys. Rev. D*, 92:019903, Jul 2015.
[9] A. Aab et al. Data-driven estimation of the invisible energy of cosmic ray showers with the Pierre Auger Observatory. *Submitted to Phys. Rev. D*, 2019.
[10] A. Haungs et al. The KASCADE Cosmic-ray Data Centre KCDC: granting open access to astroparticle physics research data. *The European Physical Journal C*, 78(9):741, Sep 2018.
[11] Javier G. Gonzalez. Muon Measurements with IceTop. *EPJ Web Conf.*, 208:03003, 2019.
[12] T Antoni et al. The cosmic-ray experiment KASCADE. *Nuclear Instruments and Methods in Physics Research Section A: Accelerators, Spectrometers, Detectors and Associated Equipment*, 513(3):490 – 510, 2003.
[13] KIT, Karlsruhe Institute of Technology. KASCADE Cosmic Ray Data Centre (KCDC). https://kcdc.ikp.kit.edu/. Accessed: 22 April 2019.
[14] D. Heck et al. Upgrade of the Monte Carlo code CORSIKA to simulate extensive air showers with energies > 10^{20} eV. *Report FZKA Forschungszentrum Karlsruhe*, 6019, 1998.
[15] KIT, Karlsruhe Institute of Technology. *KCDC User Manual*, V.17 from 2018-07-13. https://kcdc.ikp.kit.edu/static/pdf/kcdc_mainpage/kcdc-Manual.pdf.
[16] KIT, Karlsruhe Institute of Technology. *KCDC Simulation Manual*, V.01.1 from 2017-10-30. https://kcdc.ikp.kit.edu/static/pdf/kcdc_mainpage/kcdc-Simulation-Manual.pdf.
[17] T. Pierog et al. EPOS LHC: Test of collective hadronization with data measured at the CERN Large Hadron Collider. *Phys. Rev. C*, 92:034906, Sep 2015.
[18] S. Ostapchenko. Monte Carlo treatment of hadronic interactions in enhanced Pomeron scheme: QGSJET-II model. *Phys. Rev. D*, 83:014018, Jan 2011.
[19] F. Riehn et al. A new version of the event generator Sibyll. *The 34th International Cosmic Ray Conference (ICRC2015) PoS(ICRC2015)558*, October 2015.
[20] H. P. Dembinski et al. Data-driven model of the cosmic-ray flux and mass composition from 10 GeV to 10^{11} GeV. In *Proceedings of the 35th International Cosmic Ray Conference ICRC 2017, PoS(ICRC 2017)533*, 2017.
[21] H. P. Dembinski et al. Report on Tests and Measurements of Hadronic Interaction Properties with Air Showers. *EPJ Web Conf.*, 210:02004, 2019.
[22] T. Bergmann et al. One-dimensional Hybrid Approach to Extensive Air Shower Simulation. *Astropart. Phys.*, 151:159, 2006.
[23] T. Pierog et al. First results of fast one-dimensional hybrid simulation of EAS using CONEX. *Nucl. Phys. Proc. Suppl.*, 26:420, 2007.
[24] R. Abbasi and G. Thomson. $< X_{max} >$ Uncertainty from Extrapolation of Cosmic Ray Air Shower Parameters. In *Ultra-High Energy Cosmic Rays (UHECR2016)*, page 011015, 2018.

PoS(ICRC2023)497